ORCA – Online Research @ Cardiff

This is an Open Access document downloaded from ORCA, Cardiff University's institutional repository:https://orca.cardiff.ac.uk/id/eprint/122646/

This is the author's version of a work that was submitted to / accepted for publication.

Citation for final published version:

Lorenzer, Cornelia, Streußnig, Sonja, Tot, Emilia, Winkler, Anna-Maria, Merten, Hannes, Brandl, Fabian, Sayers, Edward J. , Watson, Peter , Jones, Arwyn T. , Zangemeister-Wittke, Uwe, Plückthun, Andreas and Winkler, Johannes 2019. Targeted delivery and endosomal cellular uptake of DARPin-siRNA bioconjugates: Influence of linker stability on gene silencing. European Journal of Pharmaceutics and Biopharmaceutics 141 , pp. 37-50. 10.1016/j.ejpb.2019.05.015

Publishers page: http://dx.doi.org/10.1016/j.ejpb.2019.05.015

Please note:
Changes made as a result of publishing processes such as copy-editing, formatting and page numbers may not be reflected in this version. For the definitive version of this publication, please refer to the published source. You are advised to consult the publisher's version if you wish to cite this paper.

This version is being made available in accordance with publisher policies. See http://orca.cf.ac.uk/policies.html for usage policies. Copyright and moral rights for publications made available in ORCA are retained by the copyright holders.

ACCEPTED MANUSCRIPT

# Targeted delivery and endosomal cellular uptake of DARPin-siRNA bioconjugates: Influence of linker stability on gene silencing

Cornelia Lorenzer[a], Sonja Streußnig[a], Emilia Tot[a], Anna-Maria Winkler[a], Hannes Merten[b], Fabian Brandl[b], Edward J. Sayers[c], Peter Watson[d], Arwyn T. Jones[c], Uwe Zangemeister-Wittke[b,e], Andreas Plückthun[b], Johannes Winkler[a,f,*]

[a]Department of Pharmaceutical Chemistry, University of Vienna, Althanstraße 14, 1090 Vienna, Austria

[b]Department of Biochemistry, University of Zurich, Winterthurerstraße 190, 8057 Zurich, Switzerland

[c]Cardiff School of Pharmacy and Pharmaceutical Sciences, Cardiff University, Cardiff, Wales, CF10 3NB, United Kingdom

[d]School of Biosciences, Cardiff University, Cardiff, Wales, CF10 3AX, United Kingdom

[e]Institute of Pharmacology, University of Bern, Inselspital INO-F, 3010 Bern, Switzerland

[f]Department of Cardiology, Medical University of Vienna, Währinger Gürtel 18-20, 1090 Vienna, Austria

*corresponding author: Email: johannes.winkler@univie.ac.at

ACCEPTED MANUSCRIPT


## Abstract

Specific cell targeting and efficient intracellular delivery are major hurdles for the widespread therapeutic use of nucleic acid technologies, particularly siRNA mediated gene silencing. To enable receptor-mediated cell-specific targeting, we designed a synthesis scheme that can be generically used to engineer Designed Ankyrin Repeat Protein (DARPin)-siRNA bioconjugates. Different linkers, including labile disulfide-, and more stable thiol-maleimide- and triazole- (click chemistry) tethers were employed. Crosslinkers were first attached to a 3'-terminal aminohexyl chain on the siRNA sense strands. On the protein side thiols of a C-terminal cysteine were used as anchoring site for disulfide- and thiol-maleimide conjugate formation, while strain-promoted azido-alkyne cycloadditions were carried out at a metabolically introduced N-terminal azidohomoalanine. After establishing efficient purification methods, highly pure products were obtained. Bioconjugates of EpCAM-targeted DARPins with siRNA directed at the luciferase gene were evaluated for cell-specific binding, uptake and gene silencing. As shown by flow cytometry and fluorescence microscopy, all constructs retained the highly specific and high-affinity antigen recognition properties of the native DARPin. As expected, internalization was observed only in EpCAM-positive cell lines, and predominantly endolysosomal localization was detected. Disulfide linked conjugates showed lower serum stability against cleavage at the linker and thus lower internalization into endosomes compared to thiol-maleimide- and triazole-linked conjugates, yet induced more pronounced gene silencing. This indicates that the siRNA payload needs to be liberated from the protein in the endosome. Our data confirm the promise of DARPin-siRNA bioconjugates for tumor targeting, but also identified endosomal retention and limited cytosolic escape of the siRNA as the rate-limiting step for more efficient gene silencing.


**Keywords**: bioconjugation; DARPins; endocytosis; siRNA; targeting



ACCEPTED MANUSCRIPT

ACCEPTED MANUSCRIPT

## Introduction

Therapeutic nucleic acid technologies for gene silencing and eventually gene editing generally suffer from insufficient delivery to their target in cytoplasm or nucleus [1]. The structural and physicochemical properties of synthetic oligonucleotides, being multiply charged hydrophilic oligomers, essentially prevent unassisted cellular uptake into any compartment [2]. Two potential solutions are currently being investigated for the delivery issue in preclinical and clinical research, namely packaging in liposomes or other nanoparticle formulations [3], or the use of bioconjugates as vehicles for receptor-mediated uptake [4].

Patisiran, a liposomal formulation of an siRNA against transthyretin (TTR) amyloidosis [5], has recently been approved by the FDA and EMA as the first siRNA reaching market authorization. The liver is the natural destination organ for particles with the characteristics and size of liposomes. A large share of the preclinical and clinical pipelines consists of siRNA and antisense conjugates with the GalNAc (N-acetyl galactosamine) ligand [6], shown to be efficiently and rapidly internalized into hepatocytes upon binding to the asialoglycoprotein receptor [7]. Although this demonstrates the applicability of receptor-mediated endocytosis for tumor targeting with nucleic acids, it is questionable whether this concept can be widely used for targeting cells other than hepatocytes [1]. Specifically, the asialoglycoprotein receptor has the unique characteristics of being expressed in high density on hepatocytes and being internalized quickly upon ligand binding with subsequent recycling back to the extracellular membrane [8, 9]. Thus, even though GalNAc conjugates are lacking a specific endosomal escape mechanism, ostensibly overloading of endosomes suffices to generate adequate cytosolic oligonucleotide concentrations for therapeutic gene silencing [10]. Additionally, GalNAc adds no charge and very little mass to the oligonucleotide.

ACCEPTED MANUSCRIPT

To employ therapeutic receptor-targeting beyond hepatocytes, both highly expressed receptors and cognate high-affinity ligands are required. Antibodies remain the gold standard for highly specific protein-protein interactions, but because of their structure, low stability, and the reliance of posttranslational modifications for correct folding, antibody derivatization and bioconjugations are complicated [11]. Designed Ankyrin Repeat Proteins (DARPins) are modular protein scaffolds which can be evolved to produce high affinity and binding specificity [12]. Having been developed from natural ankyrin proteins, the DARPin consensus framework consists of N- and C-terminal repeat domains specifically engineered for high stability, and usually three internal repeat domains, which mediate specific protein-protein interactions through randomized positions [12]. In recent years, DARPins against an increasing number of different antigens have been developed and characterized, and besides direct therapeutic development, several biochemical and pharmaceutical applications have been described [12, 13]. DARPins are particularly well suited for targeting approaches, because of the ease of derivatization and facile site-specific covalent attachment of cargoes [14-16]. For example, unique thiol groups can be introduced by a cysteine at any desired position, and strain-promoted azido-alkyne cycloaddition (SPAAC, copper-free click chemistry) is afforded by metabolic introduction of an azido-containing amino acid [17, 18]. With these modifications, controlled site-specific bioconjugation of synthetic oligonucleotides is feasible.

We previously reported the generation and use of DARPin fusion proteins for charge-mediated complexation of siRNA payloads for tumor-targeting [19]. In terms of pharmaceutical development, the DARPin bioconjugates have the advantage of being defined single molecules, which facilitates reproducibility of the assembly process, quality control, upscaling, and they have overall better pharmacokinetic properties to enhance specific delivery to the targeted

ACCEPTED MANUSCRIPT

receptor on cells [20, 21]. Oligonucleotides for intracellular gene silencing and DARPins for receptor binding on the cell surface are both modular technologies, and their conjugation is a generic process, in principle allowing substituting both the targeted cell surface receptor and the gene to be silenced by simply exchanging carrier protein and nucleic acid payload, respectively.

Here, we describe optimized strategies for the synthesis of DARPin-oligonucleotide conjugates with three distinct linker chemistries, their analytical and biochemical characterization, and the evaluation of intracellular delivery and gene silencing. To enable *in vitro* characterization under defined conditions, we used a siRNA targeted at luciferase (anti-Luc siRNA), and a well-characterized monovalent DARPin with high affinity for the pan-carcinoma marker EpCAM [22, 23]. EpCAM is overexpressed in many solid tumors and rapidly internalized upon ligand binding [18]. The ability of the various conjugates to inhibit luciferase expression and their potential cytotoxicity were examined in EpCAM-positive and negative cell lines.

## Materials and Methods

### Expression and purification of DARPins

*E. coli* XL1-Blue (Agilent Technologies, Santa Clara, CA, USA) or B834 (DE3) [17] were freshly transformed with a plasmid encoding the anti-EpCAM DARPins Ec4-C, carrying a single cysteine at the C-terminus or Ec1 for the incorporation of an N-terminal azidohomoalanine (Aha), replacing the initiator Met [22]. For Ec4-C (*E. coli* XL1-Blue), a single colony was used to inoculate LB broth or 2YT medium supplemented with 50 µg/mL ampicillin and 1.0% glucose and shaken at 37 °C overnight. The following day, 500 mL of LB broth (Sigma Aldrich, Vienna, Austria) or 2YT medium was inoculated to result in an optical density at 600 nm ($OD_{600}$) of ~0.1 and the suspension was incubated at 37 °C until an $OD_{600}$ of 0.4-0.6 was reached. Protein

ACCEPTED MANUSCRIPT

expression was induced by adding isopropyl-β-D-thiogalactopyranoside (IPTG, final concentration 0.5 mM; Thermo Fisher, Waltham, USA) and the culture was shaken at 37 °C for 4 h.

For the expression of Aha-modified Ec1 in *E. coli* B834 (DE3), Pre-M9 medium (SelenoMet basal medium (Molecular Dimensions) with 40 mg/L L-methionine, 5% (v/v) glucose-free nutrient mix (Molecular Dimensions), 50 mg/L ampicillin, and 1% (w/v) glucose), was inoculated with a single colony of transformed bacteria. The next day, 500 mL Pre-M9 medium was inoculated to an $OD_{600}$ of ~0.1 and the bacterial suspension was shaken at 37° C until an $OD_{600}$ of 1.0-1.2 was reached. The culture was subsequently centrifuged (Eppendorf, Vienna, Austria) at 4 °C for 15 min and washed thoroughly three times by resuspending the pellet in ice-cold PBS followed by centrifugation. The remaining pellet was transferred into M9 medium (SelenoMet basal medium with 40 mg/L L-azidohomoalanine (H-Dab($N_3$)·HCl, Bapeks, Riga, Latvia), 5% (v/v) nutrient mix, 50 mg/L ampicillin, and 0.4% (w/v) glycerol. The bacterial culture was agitated for 15 min at 30 °C, then expression was induced with 1 mM IPTG followed by incubation at 37°C for 4 h. Thereafter, bacteria were collected by centrifugation at 4,000 rpm for 20 min. The pellets were dried and stored at -80 °C.

After thawing, each pellet was resuspended in 30 ml of 20 mM HEPES, 500 mM NaCl, 25 mM imidazole, pH 8.0 and a spatula tip of lysozyme was added and the solution was incubated for 30 min. The solution was thoroughly sonicated with cooling between sonication cycles until the cells were disrupted. The lysate was centrifuged for 30 min at 16,000 x g and the supernatant was loaded into PD-10 columns packed with Ni-NTA resin (Qiagen, Hildesheim, 1 ml per 10-30 mg protein), which had been equilibrated with 20 mM HEPES, 500 mM NaCl, 25 mM imidazole, pH 8.0. After supernatant loading, the column was washed with 10 column volumes 20 mM

ACCEPTED MANUSCRIPT

HEPES, 500 mM NaCl, 25 mM imidazole, pH 8.0 and the protein eluted using 20 mM HEPES, 500 mM NaCl, 300 mM imidazole, pH 8.0. During the elution, fractions of 0.5-1 ml were collected. Protein containing fractions were pooled and dialyzed against PBS. For Ec4-C, all buffers contained 5 mM DTT.

**siRNA**

All fluorescently labelled and unlabelled siRNAs were synthesized at GlaxoSmithKline (GSK, Stevenage, UK). For all bioconjugates, a siRNA complementary to luciferase mRNA (anti-Luc siRNA) was used (sense strand, CUUACGCUGAGUACUUCGA-PS-dT-PS-dT with a 3'-aminohexyl linker, antisense strand, UCGAAGUACUCAGCGUAAG-dT-PS-dT; underlined nucleotides are 2'-*O*-methylated, PS indicates phosphorothioate bonds).

**Attachment of crosslinkers to 3'-aminohexyl sense strands**

The sense strand of 3' aminohexyl-modified anti-Luc siRNA was dissolved in nuclease free water (Sartorius arium® pro, Göttingen, Germany) to give a 1 mM solution. For generation of the disulfide-linked bioconjugate, the succinimidyl 3-(2-pyridyldithio)propionate (SPDP, Thermo Scientific, Waltham, USA) crosslinker was dissolved in anhydrous dimethyl sulfoxide (DMSO; Sigma Aldrich, Vienna, Austria) to a 20 mM solution. A 5-fold molar excess of SPDP crosslinker (500 nmol) was added to the solution of the sense strand (100 nmol) and the reaction was buffered to a final concentration of 47 mM sodium phosphate buffer (Gibco, Life Technologies, Carlsbad, USA), adjusted to pH 8.5. The solution was mixed gently for 1 hour at 25 °C. The excess of SPDP crosslinker was removed by precipitation of the SPDP-crosslinked anti-Luc siRNA with 2-propanol and centrifugation at 13,000 x g for 10 min at 4 °C. The pellet was washed three times with 75% ice-cold ethanol and finally dissolved in nuclease-free water.

ACCEPTED MANUSCRIPT

For the preparation of thiol-maleimide-linked bioconjugate, sulfosuccinimidyl 4-(N-maleimidomethyl)cyclohexane-1-carboxylate (Sulfo-SMCC; Thermo Fisher, Waltham, USA) crosslinker was dissolved in nuclease free water to a 10 mM solution. A 50-fold molar excess of Sulfo-SMCC (5 µmol) was added to the sense strand of 3'-aminohexyl-anti-Luc siRNA (100 nmol) in 47 mM sodium phosphate buffer, adjusted to pH 7.7 and mixed at 25 °C for 3 h.

For the synthesis of the dibenzocyclooctyne (DBCO)-crosslinked siRNA sense strand, a 10 mM solution of DBCO-NHS ester (Sigma Aldrich, Vienna, Austria) was prepared in DMSO. A 10-fold molar excess (1 µmol) was added to the sense strand of 3'-aminohexyl-modified anti-Luc siRNA (100 nmol) and the reaction was buffered with 47 mM sodium phosphate buffer, pH 7.4. The reaction was shaken in a thermoincubator at 25 °C for 2 h. To remove the excess of linkers, thiol-maleimide- and DBCO-derivatized anti-Luc siRNA were purified by size exclusion chromatography on an ÄKTA Pure chromatography system equipped with a Superdex 75 10/300 GL column (GE Healthcare, Vienna, Austria) with elution with 47 mM sodium phosphate buffer, pH 7.4 at a flow rate of 0.5 mL/min. Fractions containing derivatized sense strand of siRNA were collected, pooled and concentrated to a 100 to 200 µM solution with 3 kDa Amicon centrifugal filters (Merck Millipore, Darmstadt, Germany).

**Reversed Phase High performance liquid chromatography (HPLC)**

All oligonucleotide-crosslinker reactions were monitored by RP-HPLC measurements (Shimadzu, Korneuburg, Austria) on a reversed phase column for oligonucleotide analysis (Clarity 5 µ RP18 250 x 4.60 mm, Phenomenex, Torrance, USA). For all runs, a 60 min linear gradient of 8-44% acetonitrile in triethylammonium acetate (TEAA) buffer in nuclease-free water, adjusted to pH 7.0 was performed at a flow rate of 1 mL/min. Before RP-HPLC measurement, 25 mM dithiothreitol (DTT) was added to SPDP-crosslinked siRNA sample for

ACCEPTED MANUSCRIPT

disulfide cleavage. All siRNA samples were diluted to a 50 µM solution with TEAA buffer for measurements.

**Electrospray ionization mass spectrometry (ESI-MS)**

Samples for ESI-MS measurements were purified as published [24]. To this end, 30 µL of a 25 µM siRNA sample were mixed in 15 µL 7.5 M ammonium acetate solution and left at room temperature for 1 hour. After addition of 115 µL of ethanol, the samples were precipitated overnight at -80° C. The samples were centrifuged for 30 min at 12,000 x g and 0 °C to collect the oligonucleotide. After washing with 100 µL ice-cold 75% ethanol and centrifugation for 20 min at 12,000 x g and 0 °C, the pellet was air-dried and dissolved in 50 µL nuclease-free water. For MS analyses, the samples were diluted to a 10 µM solution with 10 mM ammonium acetate in RNase-free water. Since direct ESI-MS measurement of intact pyridyldithiol-oligonucleotide resulted in mulitple peaks, the disulfide bond was cleaved by DTT at a final concentration of 10 mM directly before ESI-MS measurement, which better maintained integrity. Analyses were performed on an electrospray-quadrupole time-of-flight mass spectrometer (Bruker maXis HD, Bremen, Germany). Calibration was done with ES-TOF Tuning Mix (Sigma Aldrich, Vienna, Austria) and the samples were measured in negative mode.

**Reduction of C-terminal cysteine-modified DARPin Ec4**

Cysteine-modified DARPin Ec4-C was reduced with 25 mM DTT in 20 mM Tris, 200 mM NaCl, pH 8.0 at 37 °C for 30 min. Excess DTT was removed by size exclusion chromatography in a 15 mL polypropylene column with Sephadex G50 (GE Healthcare, Vienna, Austria) and gravity flow elution with nuclease free water. Protein-containing fractions were identified by nanophotometric measurements with a NanoDrop ND-1000 instrument (Peqlab Biotechnologie

ACCEPTED MANUSCRIPT

GmbH, Erlangen, Germany) and pooled. The volume was reduced to reach a concentration between 1.0 and 2.0 mg/mL.

**Synthesis of DARPin-based siRNA conjugates**

For the disulfide-linked bioconjugate, a 2-fold molar excess of freshly reduced Ec4-C (38 nmol, 2.0 mg/mL) was added to the SPDP-sense strand (19 nmol). A guanidinium hydrochloride (GdnHCl) buffer (4.5 M GdnHCl, 20 mM Tris, pH 8.0) or a phosphate buffer (13.5 mM KCl, 9 mM $KH_2PO_4$, 685 mM NaCl, 50 mM $Na_2HPO_4$, 4.5 mM $CaCl_2$, 2.5 mM $MgCl_2$-$6H_2O$, pH 7.4) was added and the reaction was incubated at 25 °C for 24 h. For the thiol-maleimide-linked conjugate, a 2-fold molar excess of monomeric Ec4-C (64 nmol) was dissolved in phosphate buffer, added to the thiol-maleimide-crosslinked sense strand (32 nmol) and the reaction was incubated at 25 °C for 24 h. The DBCO-linked conjugate was generated by adding a 2-fold molar excess of Aha-Ec1 (60 nmol, 10.5 mg/mL) buffered in phosphate buffer, pH 7.4 to the DBCO-modified sense strand (30 nmol) and the reaction was incubated at 25 °C for 3 h.

**Purification of bioconjugates**

To remove unreacted oligonucleotide, Ni-NTA agarose was added to the reaction mixtures and incubated under shaking at room temperature for 30 min. The slurry was transferred into a spin column (Pierce, Waltham, USA) and washed with 1x DPBS until no siRNA was detected by nanophotometric measurements (260 nm absorption maximum). Unreacted Ec4-C and conjugate were eluted with 250 mM imidazole in nuclease-free water and the respective fractions were pooled.

For separation of unreacted protein, oligonucleotide-based affinity chromatography was used. A synthetic 3' biotinylated 2'-desoxy-oligonucleotide (AGCATCAGTCGCGTAAG) with partial

ACCEPTED MANUSCRIPT

complementarity to the siRNA strand was immobilized on streptavidin sepharose (GE Healthcare, Vienna, Austria). The conjugate was applied to the immobilized DNA and unreacted protein was removed by washing with ice-cold high salt buffer (2x DPBS). The conjugate was eluted in low-salt buffer (0.4 mM KCl, 0.2 mM $KH_2PO_4$, 20.0 mM NaCl and 1.2 mM $Na_2HPO_4$, pH 7.4) at 35 °C.

**Duplex formation**

Equimolar amounts of DARPin-single strand siRNA conjugate and the corresponding antisense strand either with or without Alexa Fluor 568 label at a 3'-aminohexyl linker were mixed in nuclease-free water. For verifying complete hybridization, an aliquot of the mixture (20 pmol) with labelled antisense was incubated at room temperature for 10 min or at 60 °C for 5 min. After incubation, samples were mixed with DNA loading dye (0.01% bromophenol blue, 20% sucrose) and analyzed on a 20 % native acrylamide gel (7.5 mL 40% 29:1 acrylamide:bisacrylamide, 1.5 mL 10x TBE buffer, 6.0 mL water, 7.5 µL tetramethylethylene diamine, 75 µL 10 % ammonium persulfate). The gel was run in 1x TBE buffer at 100 V for 90 min, digitalized in a Ettan Dige Imager (GE Healthcare, Vienna, Austria) and analyzed with ImageQuant™ TL software.

**Stability test and agarose gel electrophoresis**

Disulfide-, thiol-maleimide- and DBCO-linked conjugates were incubated in DMEM with 10% FBS at 37 °C for 0 h, 1 h, 3 h, 24 h and 48 h (Thermomixer, Eppendorf). Samples were analyzed on a 2% agarose gel with a final concentration of 0.5 µg/mL ethidium bromide. The gel was scanned in a ChemiDoc™ XRS gel imaging system (Bio-Rad, Vienna Austria,) and analyzed using the QuantityOne Software (Bio-Rad, Vienna, Austria).

ACCEPTED MANUSCRIPT

**Cell culture**

HeLa, MDA-MB-468, and MCF-7 cell lines were obtained from the European Collection of Authenticated Cell Cultures (ECACC). Cells were cultivated in Dulbecco's Modified Eagle Medium (DMEM) + GlutaMax™ (Gibco, Carlsbad, USA) supplemented with 10% FBS (Gibcoat 37 °C and 5% $CO_2$. For passaging cells were washed with pre-warmed PBS, trypsinized with TrypLE™ Express (Gibco), and resuspended in pre-warmed medium.

**EpCAM-specific binding activity of bioconjugates**

Antigen-specific binding activity was tested by flow cytometry on EpCAM-positive MDA-MB-468 cells and EpCAM-negative HeLa cells. After trypsinization and resuspension in DMEM (10% FBS), cells were counted in a Thoma chamber. Cells were washed with 3 mL PBS and centrifuged for 10 min at 4 °C and 200 x g (Eppendorf, Vienna, Austria). The supernatant was removed and the cells were resuspended in the appropriate volume of FACS buffer (PBS with 1% FBS) to give a density of 1.2 x $10^6$ cells/mL. The indicated amount of bioconjugate (330 or 1330 nM), Ec4-C or Aha-Ec1 was added to 1.8 x $10^5$ MDA-MB-468 or HeLa cells and the mixture was incubated for 1 h on ice. Afterwards cells were washed twice with 1 mL FACS buffer, centrifuged for 10 min at 4 °C/100 x g and the supernatant was removed. Cells were resuspended in 200 µl FACS buffer containing 2 µl anti-penta·His Alexa 488 mouse IgG1 (Qiagen, Hilden, Germany) and incubated on ice for 1 h. After washing twice, the cells were resuspended in 500 µl ice-cold FACS buffer, cooled on ice and immediately analyzed by flow cytometry. The same procedure except incubation with the anti-penta His antibody was carried out with Alexa Fluor 568 labelled conjugates at 330 and 1330 nM.

On a BD FACSCalibur™ flow cytometer (BD Bioscience, San Jose, USA), $10^4$ cells per sample were analyzed with the filter settings for the respective fluorophores. Results were

ACCEPTED MANUSCRIPT

quantified by BD CellQuest™ (BD Bioscience, San Jose, USA) and FlowJo (FlowJo LLC, Ashland, USA) software.

**EpCAM-specific uptake studies**

EpCAM-specific uptake of siRNA containing an Alexa Fluor 568 labeled antisense strand, was investigated by flow cytometry and confocal microscopy on EpCAM-positive MDA-MB-468 cells and EpCAM-negative HeLa cells. For flow cytometry, cells were seeded in a 24-well plate at a density of $10^5$ cells in 200 µL. Cells were cultured under standard conditions for 24 h. The medium was removed, and the bioconjugates (330 and 1330 nM) as well as controls diluted in DMEM with 10% FBS were added and cells were incubated for 24 h. The medium was removed, cells were washed twice with 500 µL FACS buffer, and trypsinized. The cells were resuspended in 500 µL FACS buffer, cooled on ice and immediately analyzed as described above.

Cell specific uptake and intracellular trafficking of bioconjugates were monitored on MCF-7 and HeLa cells by confocal microscopy. Per 35 mm imaging dish (MatTek, Ashland, MA, USA) 2 x $10^5$ cells (21,000 cells/$cm^2$) HeLa and 3 x $10^5$ cells per dish (32,000 cells/$cm^2$) MCF-7 were seeded and incubated for 48 h under tissue culture conditions. For uptake experiments in MCF-7 and HeLa, cells were incubated with 200 µL of bioconjugate (400 nM) in DMEM/10% FBS for 6 h before washing in imaging medium (phenol-red-free DMEM/20 mM HEPES (Gibco) and 10% FBS) and imaged by confocal microscopy. For analyzing binding and uptake, MCF-7 cells were pre-chilled on ice for 15 mins before incubating with ice cold 200 µL of bioconjugate (400 nM) in DMEM/10% FBS for 1 h. Cells were subsequently washed in ice-cold imaging medium and imaged by confocal microscopy. After imaging, cells were returned to 37 °C/5% $CO_2$ for 2 h before re-imaging by confocal microscopy. To assess lysosomal localization, MCF-7 cells were incubated with 0.1 mg/mL Alexa Fluor 488 dextran conjugate (Life Technologies) for

ACCEPTED MANUSCRIPT

2 h in medium containing 10% FBS. Cells were subsequently washed and reincubated in fresh serum containing medium overnight to allow the dextran probe to reach a terminal endocytic compartment. Cells were subsequently incubated with 400 nM of bioconjugates in medium containing FBS (final volume 200 µL) for 6 h before washing and imaging by confocal microscopy in imaging medium containing 5 µg/mL Hoechst 33342.

Confocal microscopy was performed on a Leica SP5 LCSM using 60x 1.4NA objective, 488 nm Argon and 543 nm HeNe lasers with a raster size of 1024 x 1024 giving a pixel size of 96.1 $nm^2$ at a depth of 8 bits.

**Luciferase reporter assay**

We used MCF-7 and HeLa cells transduced with a lentiviral vector encoding a PGK-EGFP-Luc cassette as described previously [25], the mRNA of which is complementary to the antisense strand of the anti-Luc siRNA. To ensure that the conjugates are able to induce gene silencing after reaching the cytosol, Lipofectamine RNAiMAX was used for transfecting DARPin-conjugates as well as the unconjugated siRNA. The indicated amounts of bioconjugates or siRNA diluted in 20 µL Opti-MEM (Gibco, Carlsbad, USA) were transferred into corresponding wells of a white 96-well plate (Greiner Bio-One, Kremsmünster, Austria) and 2.5 x $10^4$ MCF-7 or 2.0 x $10^4$ HeLa cells in 80 µL per well were added in DMEM with 10% FBS. For some experiments, cells were co-incubated with 1 µM conjugates and 62.5 µM chloroquine. After 48 h incubation, the medium was removed and cells were washed with 100 µL pre-warmed PBS. Passive lysis buffer (20 µL; Promega, Mannheim, Germany) was added to each well and cells were lysed for 30 min at RT with gentle shaking. Luciferin substrate (100 µL per well; 3.0 mg/mL luciferin in 20 mM glycylglycine, pH 7.8, 1 mM $MgCl_2$, 1 mM EDTA, 3.3 mM DTT, 0.5 mM ATP, 0.3 mM coenzyme A) was added via the plate reader's injector and luminescence signals were measured

ACCEPTED MANUSCRIPT

immediately (Tecan infinite M200Pro, Tecan, Grödig, Austria). The relative gene knockdown was calculated relative to untreated cells. Statistical significance was calculated by one-way ANOVA with Bonferroni post-hoc correction, and p-values <0.05 were considered significant.

**Viability assay**

The EZ4U proliferation assay (Biomedica, Austria, Vienna) was used for determination of cell viability after incubation of MCF-7 and HeLa cells with bioconjugates. Bioconjugates (20 µL) were transferred into a 96-well plate at a concentration of 5, 3 and 1 µM, and 2 x $10^4$ MCF-7 or 1.5 x $10^4$ HeLa cells in 80 µL per well were added in DMEM/10% FBS. Cells were incubated for 24 h at 37 °C and 5% $CO_2$. After 24 h incubation, the medium was discarded and EZ4U substrate, prepared according to the manufacturer's instructions, was added to each well. The absorbance was measured at 470 nm in a plate reader (Tecan infinite M200Pro) at 15 minutes intervals until the absorbance of untreated samples had reached 2.0. Additionally, the absorbance at 650 nm was measured as reference. The relative viability was calculated normalized to untreated cells. Statistical significance was calculated by one-way ANOVA with Bonferroni post-hoc correction, and p-values <0.05 were considered significant.

ACCEPTED MANUSCRIPT

ACCEPTED MANUSCRIPT

## Results

### Synthesis, purification and analysis of pyridyldithiol-, Sulfo-SMCC- or DBCO-crosslinked oligonucleotides

In order to synthesize bioconjugates linked with a disulfide, thiol-maleimide or triazole bond between DARPin and siRNA, the siRNA sense strand was tethered to the respective bifunctional crosslinkers, which were in turn linked to an engineered protein thiol. Accordingly, 3' amino-modified anti-luciferase siRNA sense strands were reacted with N-succinimidyl 3-(2-pyridyldithio)propionate (SPDP), sulfosuccinimidyl 4-(N-maleimidomethyl)cyclohexane-1-carboxylate (Sulfo-SMCC) and dibenzocyclooctyne (DBCO) crosslinkers, respectively (Figure 1). All reactions were carried out in amine-free aqueous buffer solutions with separately optimized pH values of 7.4 or 7.7 with a 10- to 50-fold molar excess of crosslinkers, achieving high yields under these conditions. For removing unreacted crosslinkers and other side products, thiol-maleimide-crosslinked sense siRNA was purified by size exclusion chromatography (SEC) on a Sephadex column. Partial cleavage of the disulfide of pyridyldithiol-oligonucleotide and limited solubility of DBCO-oligonucleotide in aqueous buffers hampered yields after SEC, and thus the respectively modified oligonucleotides were instead purified by precipitation from a mixture of sodium acetate and isopropanol.

HPLC analyses demonstrated that the reaction of anti-Luc siRNA sense strand (rt = 15.6 min) with the three crosslinkers yielded a nearly complete conversion to pyridyldithiol- (rt = 27.5 min), thiol-maleimide- (rt = 24.7 min) or DBCO-crosslinked (rt = 33.3 min) sense strand in 1 to 3 h reaction time (Figure 2). In addition, the removal of side products by size exclusion chromatography or precipitation was confirmed, and the large peak of the NHS hydrolysis product at rt = 3 min that was detected in reaction mixtures was absent after purification.

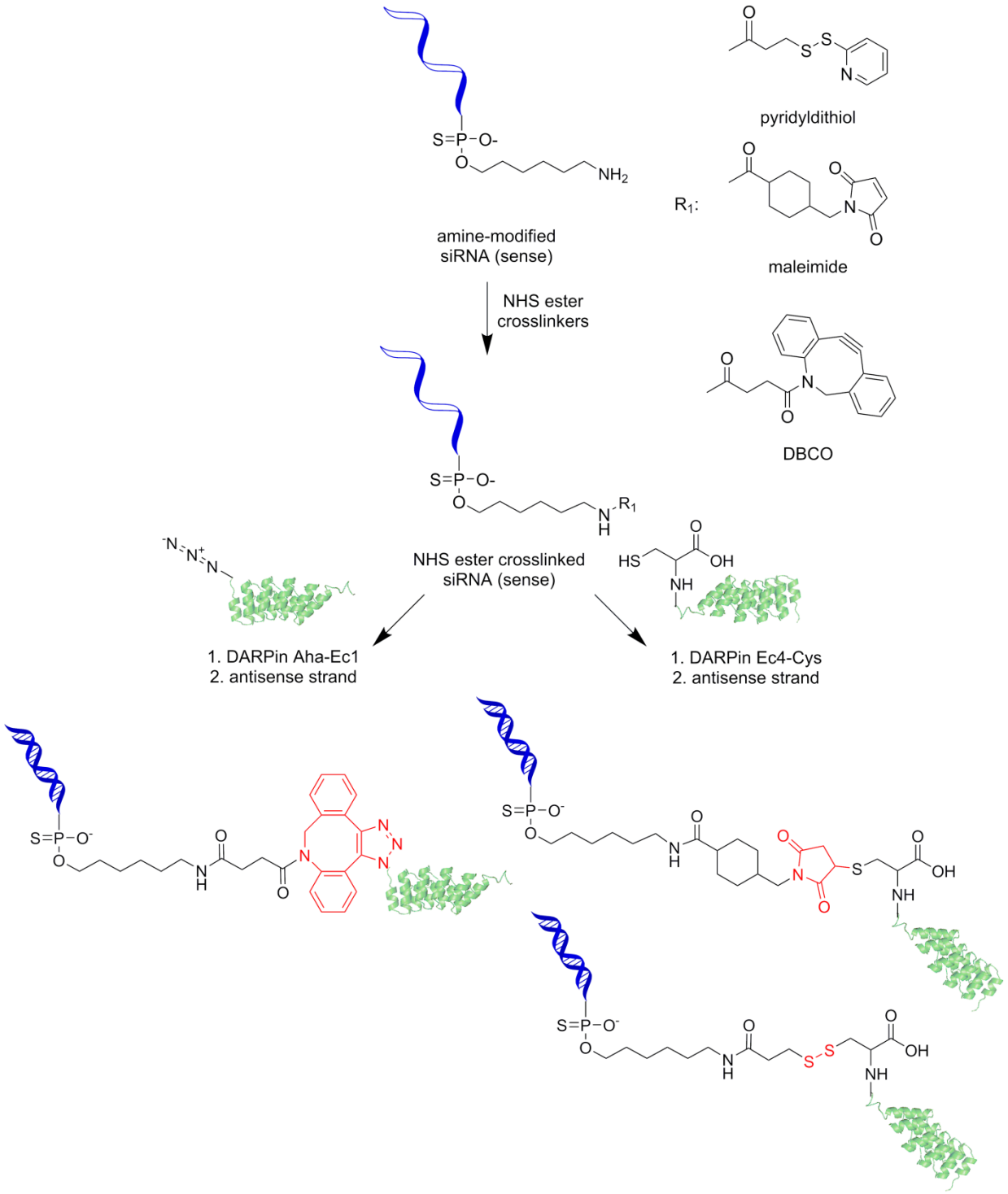


*Figure 1: Conjugation scheme. The N-hydroxy succinimide ester derivatives of SPDP, Sulfo-SMCC or DBCO linkers were tethered to 3' aminoalkyl siRNA sense strands. After purification,*

ACCEPTED MANUSCRIPT

*the DARPins (with unique L-azidohomoalanine or cysteine for site-specific conjugation) were attached to yield bioconjugates of single stranded oligonucleotides with the proteins. siRNA duplexes were then generated by adding an equimolar amount of the antisense strand and incubation at room temperature.*

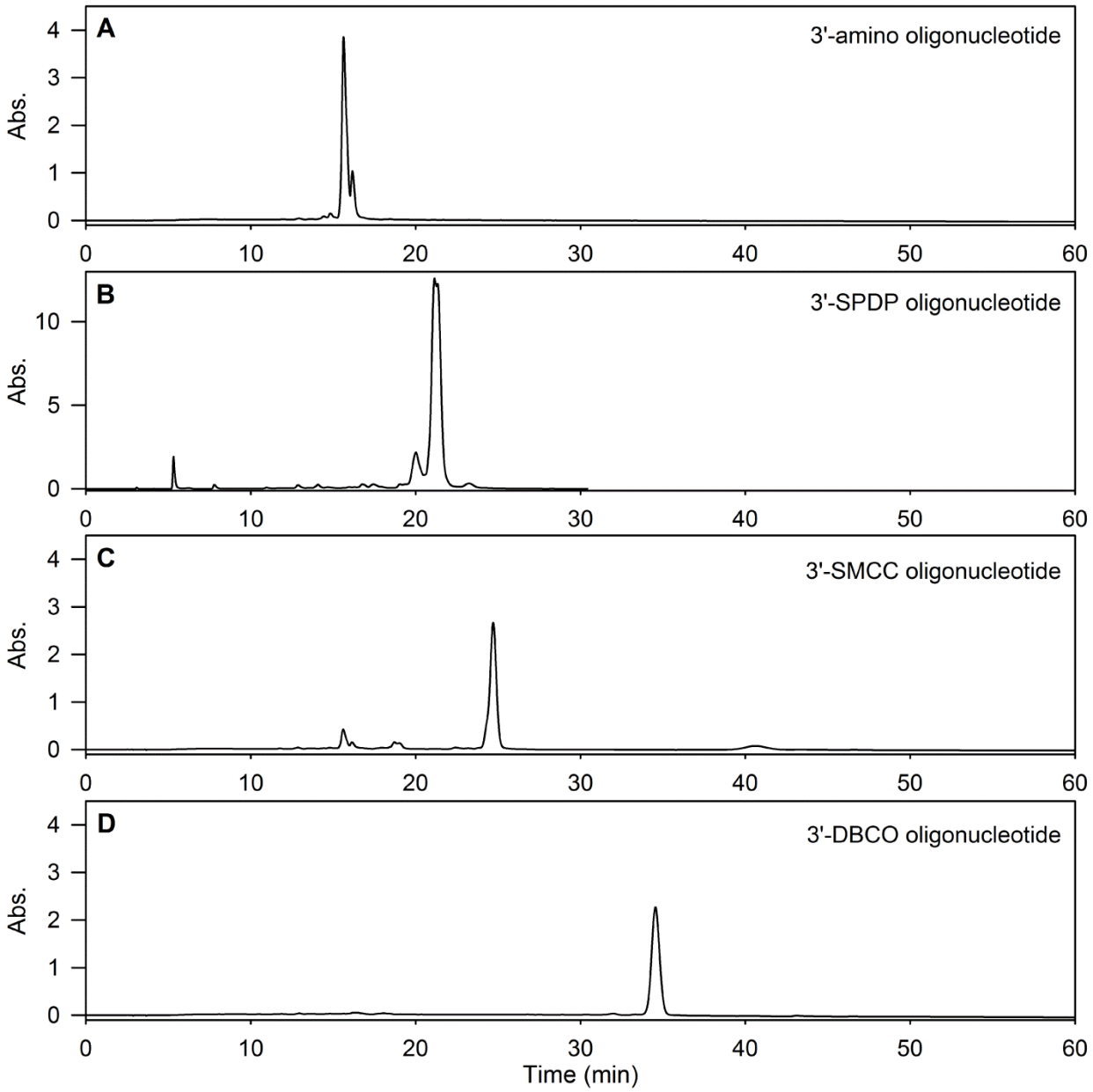

ACCEPTED MANUSCRIPT

*Figure 2: RP-HPLC analyses of amine-modified anti-Luc siRNA (A) and purified pyridyldithiol- (B), thiol-maleimide- (C) and DBCO-crosslinked (D) siRNA sense strands. Separations were achieved on a reversed phase C-18 column. A linear gradient of 8-44% acetonitrile in triethylammonium acetate (TEAA) buffer during 60 min was applied at a flow rate of 1 mL/min.*

The yields of purified siRNAs with linkers were 44% (thiol-maleimide after SEC), 63 % (DBCO after precipitation, 36 % after SEC), and 84% (pyridyldithiol after precipitation), indicating variable loss of product depending mainly on the purification method. ESI-MS measurements are consistent with the masses of all crosslinked siRNA sense strands (Table 1 and Supplementary Figure 2). Since attempts with the intact pyridyldithiol-oligonucleotide showed predominantly degradation products, the disulfide bond was intentionally reductively cleaved prior to MS to obtain cleaner spectra. Partial substitution of one sulfur of the phosphorothioate backbone by oxygen either during synthesis or MS ionization [26] resulted in a minor byproduct of pyridyldithiol siRNA.

| Oligonucleotide | Mass calculated | Mass found |
|---|---|---|
| pyridyldithiol (reduced) | 7073.07 Da | 7073.04 Da, 7057.06 Da |
| thiol-maleimide | 7207.85 Da | 7208.10 Da |
| DBCO | 7272.16 Da | 7272.12 Da |

***Table 1.*** *ESI-MS analysis of SPDP-, thiol-maleimide- and DBCO-modified siRNA sense strands*

ACCEPTED MANUSCRIPT

**Synthesis of DARPin-based siRNA bioconjugates**

For generating siRNA-bioconjugates, we used the EpCAM-specific DARPins Ec4 and Ec1, which differ only by few amino acids and have largely the same binding characteristics, including binding to the identical epitope [22]. Detailed characterization of binding has been described previously [17, 18, 22]. All conjugation reactions (Figure 1) were individually optimized through reaction monitoring by gel electrophoresis and HPLC.

Initially, reactions were carried out in native buffers with equimolar ratios of proteins and oligonucleotides. Reaction monitoring showed conversion to a product with a molecular weight corresponding to the expected conjugate. However, even after reaction times of over 24 h, both oligonucleotide and protein educts were still present, and in the case of cysteine-modified DARPin, dimerization occurred with increased reaction times, which prevents full protein conversion. In order to facilitate purification, we then conducted reactions with a two-fold excess of protein, which allowed full consumption of the oligonucleotide in maleimide-thiol and SPAAC reactions within 24 h, indicated by a shift of the peak in HPLC analyses without detectable oligonucleotide educt (Figure 3 E and F). However, the preparation of the disulfide conjugate by reaction of the pyridyldithiol oligonucleotide failed to result in complete conversion of the oligonucleotide, and with increasing reaction time, a number of side products were formed (data not shown). An increase of the formation of the desired disulfide bioconjugate was achieved by using a denaturing buffer with 4.5 M GdnHCl within a reaction time of 24 h. Since denaturation of DARPins requires high concentrations of up to 5 M of denaturing reagents and high temperatures, these conditions did not lead to complete denaturation of DARPin [13, 27]. The incomplete reaction under native conditions was attributed to the lability of the pyridyldithiol function, which also complicated MS analysis (see above). The increase in yield by GndHCl

supplementation might be caused by better access to the protein coupling site or by the high salt concentration for reduced charge expulsion between the reactants, thus favoring the conjugation reaction before linker cleavage.

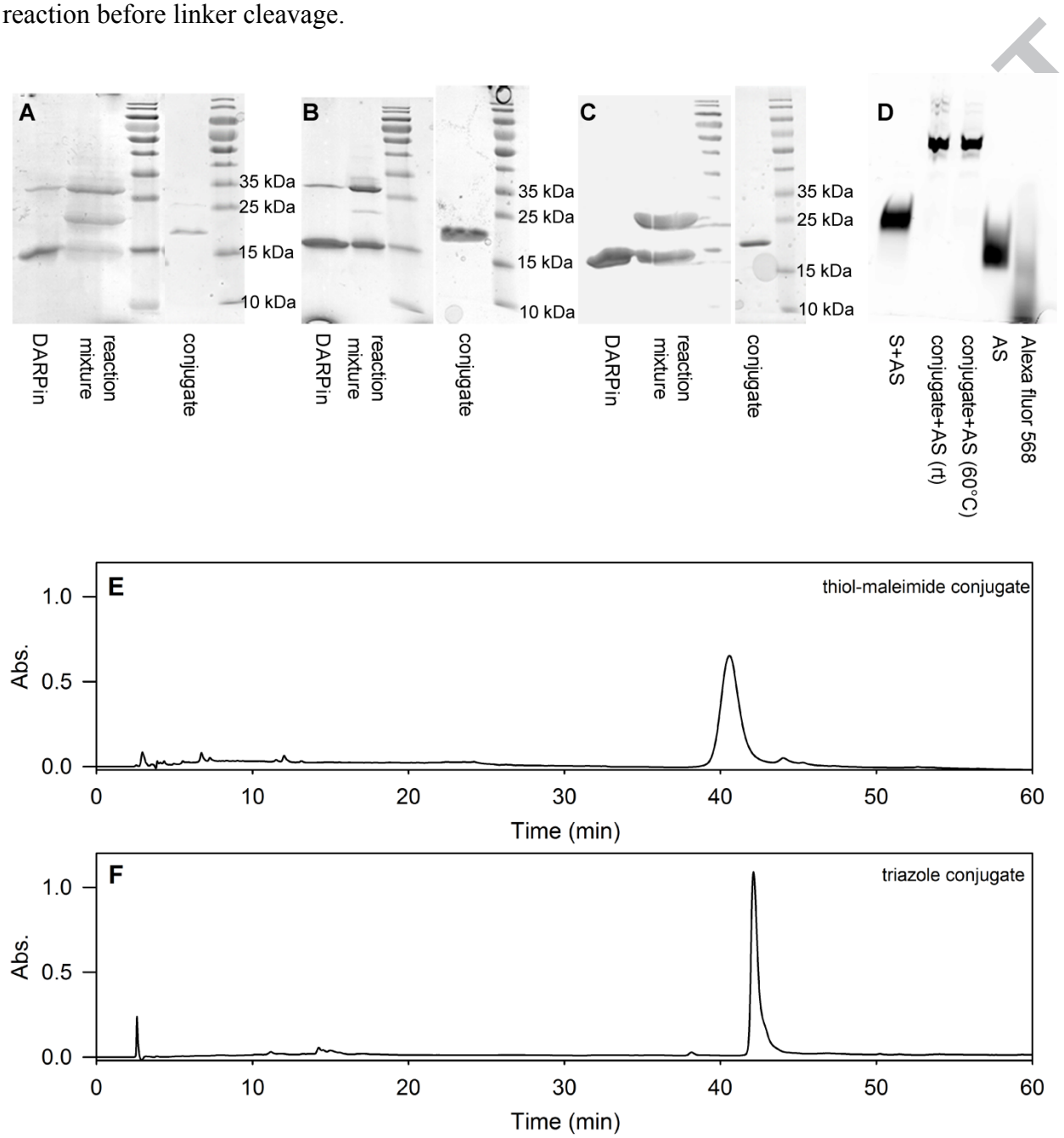


*Figure 3 Reaction monitoring of bioconjugate syntheses by gel electrophoresis (A-C) and HPLC (E and F), and duplex association monitored by gel shift assay (D). A-C: SDS*

ACCEPTED MANUSCRIPT

*polyacrylamide gels were loaded with protein samples, reaction mixtures, and purified conjugates, and stained with Coomassie blue. Disulfide-linked DARPin-oligonucleotide conjugate (26.1 kDa) after 24 h reaction at rt (A), thiol-maleimide-linked DARPin-oligonucleotide conjugate (25.9 kDa) after 3 h at rt (B), and triazole-linked DARPin-oligonucleotide conjugate (25.6 kDa) after 3 h at rt (C), all with unreacted DARPin (18.9 kDa for A and B and 18.3 kDa for C) and purified bioconjugate as indicated. The DARPin Ec4-C dimerizes under the reaction conditions, which limits the conjugation yield. D: Hybridization of Alexa Fluor 568 tagged antisense strand to DARPin-sense strand conjugates and analysis on a native polyacrylamide gel with fluorescence detection. The tagged antisense strand was added to the corresponding sense strand or to the disulfide DARPin-oligonucleotide conjugate, incubated at rt for 10 min or at 60 °C for 5 min. As controls, an siRNA duplex, the antisense single strand and free Alexa Fluor 568 dye were analyzed. The absence of a band of free antisense strands in lanes 2 and 3 proves complete hybridization to the DARPin-sense strand conjugate. E, F: RP-HPLC traces of thiol-maleimide DARPin-oligonucleotide conjugate reaction mixture (E) and triazole DARPin-oligonucleotide conjugate reaction mixture (F) showing conjugate formation and absence of oligonucleotide educts; unreacted proteins failed to elute during the gradient run. Analytical HPLCs were conducted on a reversed phase C-18 column with a linear gradient of 8-44% acetonitrile in triethylammonium acetate (TEAA) buffer during 60 min at a flow rate of 1 mL/min.*

As expected, gel electrophoresis analyses showed that disulfide-linked and thiol-maleimide-linked bioconjugate samples were separated in three bands each representing unreacted monomeric Ec4-C at 18 kDa, dimeric Ec4-C (36 kDa) and the siRNA-Ec4 conjugate at 25 kDa. Triazole-linked conjugate separation resulted in a band of unreacted Aha-Ec1 at 18 kDa and a

ACCEPTED MANUSCRIPT

band representing the DARPin-siRNA conjugate at 25 kDa (Figure 3). Unlike for the triazole conjugate, attempts to purify the disulfide- and thiol-maleimide linked conjugates by semi-preparative HPLC resulted in low product recovery, and thus we resorted to a two-step-affinity purification strategy for removing excess educts. First, unreacted oligonucleotides were removed by capturing His-tag containing compounds on a Ni-NTA resin. In order to remove unreacted DARPins, we developed an oligo-based affinity chromatography. While unconjugated Ec4-C was eluted in high-salt buffer, the conjugate was effectively bound to an immobilized oligonucleotide with partial complementarity (7 nucleotides) to the siRNA sense strand. The conjugate was then eluted in low-salt buffer. On the other hand, DBCO-linked DARPin-oligonucleotide conjugate was successfully purified by semi-preparative RP-HPLC. After purification, all bioconjugates showed high compound homogeneity, with a single band at 25 kDa, and no remnants of uncoupled proteins detected on SDS-polyacrylamide gels (Figure 3 A-C).

Conjugation yields were determined by measuring absorption at 260 nm, the absorbance maximum of oligonucleotides. The final yields after purification were 30% (disulfide), 35% (thiol-maleimide) and 47% (triazole) for conjugation reactions starting with 30-40 nmol oligonucleotide. As only minor amounts of oligonucleotide starting material was found in reaction mixtures (Figure 3), the majority of product loss occurred during purification of the relatively small amounts of bioconjugates.

**Formation of double-stranded DARPin-siRNA bioconjugates and degradation in serum**

After successful covalent attachment of the sense strand to the targeting protein, the siRNA was completed by hybridization of the antisense strand to the conjugates. Complete duplex formation was verified on a native polyacrylamide gel (Figure 3D). Due to the increased molecular weight and less negative charge-to-mass ratio, the double-stranded conjugate migrated

ACCEPTED MANUSCRIPT

more slowly than double-stranded anti-Luc siRNA, the single strand or the unattached dye. A single incubation step of 10 min at room temperature was sufficient for complete duplex formation based on Watson-Crick base pairing, indicating that the attachment of the DARPin did not influence the hybridization capability of the nucleic acids strands (Figure 3D), and a heating-cooling cycle is not required for efficient duplex formation.

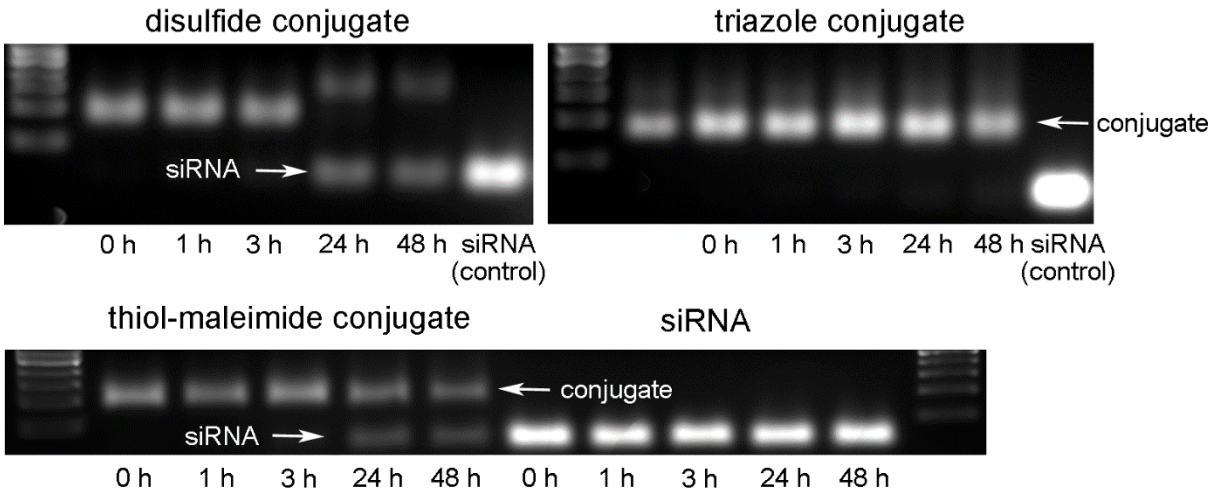


*Figure 4: Agarose gel electrophoretic analyses show different time-dependent cleavage of conjugates at the linker, releasing double stranded siRNA, in 10 % FBS in DMEM at 37 °C.*

The stability of DARPin-siRNA conjugates was evaluated in cell culture medium supplemented with 10% FBS at 37 °C. Degradation of the disulfide conjugate was observed within 24 h, with a band appearing at the size of full-length siRNA. This indicates at least partial reductive cleavage at the linker site through glutathione present in FBS (Figure 4). Thiol-maleimide- and triazole- conjugates exhibit higher stability and only minor degradation occurred during 48 h. A slow reverse reaction of the thiol-maleimide bonds under physiological conditions

ACCEPTED MANUSCRIPT

has been described before [28]. Being stabilized by chemical modifications, the siRNA itself was not readily cleaved by serum nucleases.

**EpCAM-specific binding activity**

Specific binding activities of the bioconjugates to EpCAM-positive and EpCAM-negative cell lines were analyzed by flow cytometry after incubation at 4°C (Figure 5). To ensure both cell association and bioconjugate integrity, we evaluated binding by two fluorescent reporters: a protein-specific penta-His antibody and a labelled siRNA antisense strand. As shown in Figure 5, on MDA-MB-468 cells all conjugates showed strong cell association. For disulfide and thiol-maleimide conjugates, binding signals detected by the penta-His antibody were identical to those of the unmodified DARPin. Cellular association of the triazole conjugate was considerably lower. However, no significant change in signal was encountered between the conjugates when cell association was detected through a fluorescently labelled siRNA cargo. Therefore, the reduced signal of the His-tag antibody is obviously caused by an interference of the antibody-protein binding instead of weaker binding of the conjugate to cells. In contrast to oligonucleotide attachment via the C-terminal thiol, tethering of the cargo to the N-terminal azido group adjacent to the His-tag compromises accessibility for the antibody. On HeLa cells, a weak shift of the fluorescence intensity was detected for Ec4, and to a lower extent of the conjugates. This was attributed to the high target affinity of Ec4, which in this relatively high concentration is able to bind also to cells with minimal EpCAM expression, although we cannot formally rule out a small amount of unspecific binding. Flow cytometry analysis with an anti-EpCAM antibody showed a very slight association to HeLa cells (Supplementary Figure 1), in line with available transcriptomic data [29, 30].

ACCEPTED MANUSCRIPT

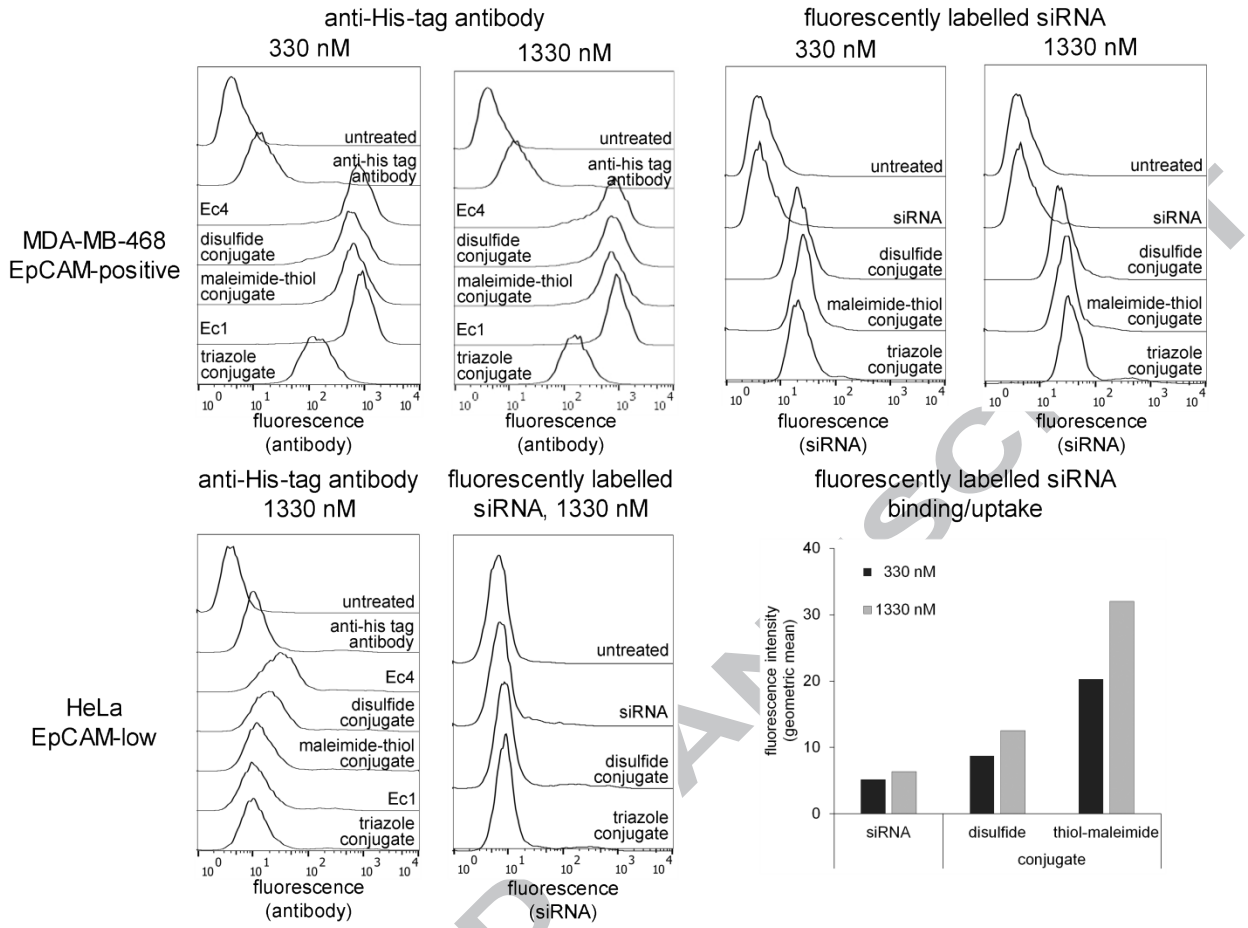


*Figure 5: Binding of conjugates to EpCAM-positive MDA-MB-468 cells and EpCAM-low HeLa cells. Conjugates and controls were incubated with cells at 4 °C for 1 h. The fluorescence signal for evaluation of EpCAM-specific protein binding was provided by the fluorescent secondary antibody anti-penta-His Alexa 488 mouse IgG1, which binds to the N-terminal His-tag of the DARPin, but is sterically blocked by the N-terminally conjugated triazole conjugate. For verification of the integrity of the conjugates and an orthogonal quantitation, the antisense strand of anti-Luc siRNA was labelled with Alexa Fluor 568 and detected in flow cytometry.*

*After incubation of EpCAM-positive MDA-MB-468 cells with bioconjugates and free siRNA in indicated concentrations for 24 h at 37° C and for providing internalization and after thorough*

ACCEPTED MANUSCRIPT

*washing to remove surface bound compounds, the fluorescence signals were quantified by flow cytometry.*

**EpCAM-specific uptake studies**

Flow cytometry analysis of bioconjugates and siRNA uptake in MDA-MB-468 cells showed a concentration-dependent cellular binding and/or uptake of disulfide-linked and thiol-maleimide-linked bioconjugates (Figure 5). However, the more stable maleimide-linked bioconjugate was associated with cells to a higher extent than the disulfide-linked DARPin-siRNA bioconjugate.

For a detailed analysis of uptake and internalization and to determine the requirement of EpCAM, we incubated the bioconjugates with EpCAM positive MCF-7 [31] and EpCAM-low control HeLa cells [29 , 30] for 6 h in complete medium (Figure 6A). A comparison between EpCAM-positive cell lines showed that MDA-MB-468 and MCF-7 cells had similar abundance of EpCAM (Supplementary Information) and thus showed similar conjugate binding, but MCF-7 resulted in slightly superior cellular uptake. Therefore, we investigated intracellular trafficking and gene silencing in MCF-7 cells. From these incubations, both thiol-maleimide and disulfide conjugates were shown to label the plasma membrane in MCF-7 cells to different extents with fluorescence, also visible in a juxtanuclear compartment. In contrast, cell-associated fluorescence was much lower in HeLa cells compared to MCF-7 with no overall intra- or extracellular localization visible. It is of interest to note that extracellular membrane localization of the disulfide linked conjugates was reduced, likely explained by the lower stability, and perhaps reducing components at the cell surface [32].

To determine a requirement for energy in the internalization of the EpCAM targeting bioconjugates, MCF-7 cells were incubated with thiol-maleimide and disulfide conjugates on ice

ACCEPTED MANUSCRIPT

for 1 h (Figure 6B). Both conjugates bound equally to the cells with no internalization or juxtanuclear labelling visible, indicating that the differences in intensity between the two bioconjugates in Figure 6A is not due to differential binding to the cell surface. Cells were subsequently warmed to 37 °C for 2 h and reanalyzed by confocal microscopy to show that internalization is an active endocytic process. Again, we detected a reduction in cell-associated fluorescence with the disulfide conjugate but not with the thiol-maleimide conjugate. This re-affirms our hypothesis that the disulfide link is being cleaved at the cell surface before the bioconjugate is fully internalized, and reducing functions at the cell surface have been described [32].

Internalized fluorescence was shown to localize to a juxtanuclear compartment and we decided to test whether the fluorescently tagged siRNA trafficked to lysosomes. Lysosomes were labelled in MCF-7 cells with dextran using a pulse-chase technique we have reported in detail previously [33]. Pre-incubation with dextran results in accumulation in LAMP1 positive lysosomes after endosomal trafficking through Rab7 positive late endosomes [34], and this protocols specifically stains lysosomes. The bioconjugates were incubated with the cells for 6 h (Figure 6 C). As seen previously, the disulfide-linked bioconjugate has far lower cell-associated fluorescence than the thiol-maleimide conjugate, however, the vast majority of the fluorescence appears to be localized to lysosomes, with very few structures not colocalizing with the dextran in this organelle. Again, the thiol-maleimide linked bioconjugate showed both internalized and plasma membrane associated fluorescence. While there are differences in the extent of internalized fluorescence within the cell population, the fluorescence signal predominately localizes to the lysosome, indicating that when either conjugate is finally endocytosed, the ultimate location of the fluorescently labeled siRNA is this organelle.

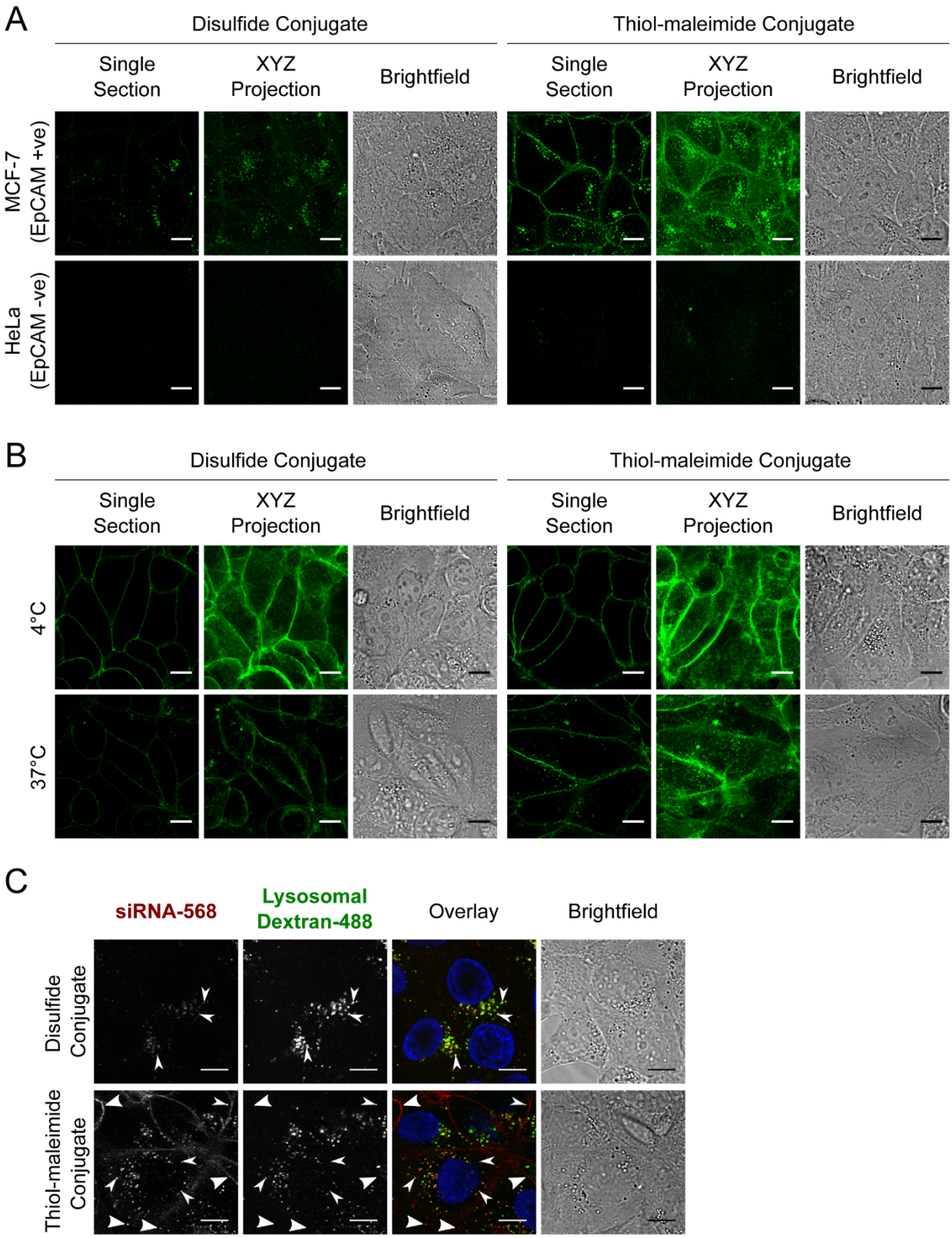
A
Disulfide Conjugate
Thiol-maleimide Conjugate
Single Section
XYZ Projection
Brightfield
MCF-7 (EpCAM +ve)
HeLa (EpCAM -ve)
B
4°C
37°C
C
siRNA-568
Lysosomal Dextran-488
Overlay
Disulfide Conjugate
Thiol-maleimide Conjugate

ACCEPTED MANUSCRIPT

*Figure 6: Cellular uptake properties of EpCAM binding bioconjugates labelled with Alexa Fluor 568 antisense strands examined by fluorescence microscopy. A, Binding and uptake of 400 nM bioconjugate in EpCAM positive (MCF-7) and EpCAM negative (HeLa) cells after 6 h continuous incubation. B, Cell surface binding of 400 nM bioconjugates incubated with MCF-7 on ice for 1 h and after a subsequent 2 h incubation at 37°. C. Dextran-488 (green) was pulsed for 2 h and chased overnight to label lysosomes, MCF-7 were incubated with 400 nM bioconjugate (red) for 6 h and imaged on the confocal microscope. Arrows indicate siRNA co-localized with lysosome, arrowheads indicate siRNA-alone. Images represent single sections, scale bars = 10 µm.*

**Luciferase reporter assay**

Reduction of luciferase gene expression was determined on respective cell lines stably expressing luciferase. Initial characterization was afforded using transient transfection of the targeted luciferase gene. However, due to varying transfection efficiency, considerable variation and poor reproducibility was encountered (data not shown), and therefore we used cell lines with stable expression of luciferase by lentiviral transduction. Since the triazole conjugates failed to show target downregulation in the transiently transfected cell lines (data not shown), we only evaluated the disulfide and thiol-maleimide conjugates in the stable luciferase expressing cell lines. To examine gene silencing after receptor-mediated internalization, disulfide- and thiol-maleimide-conjugates were applied without transfection reagent in full cell culture medium to EpCAM-positive MCF-7 and EpCAM-negative HeLa cells.

ACCEPTED MANUSCRIPT

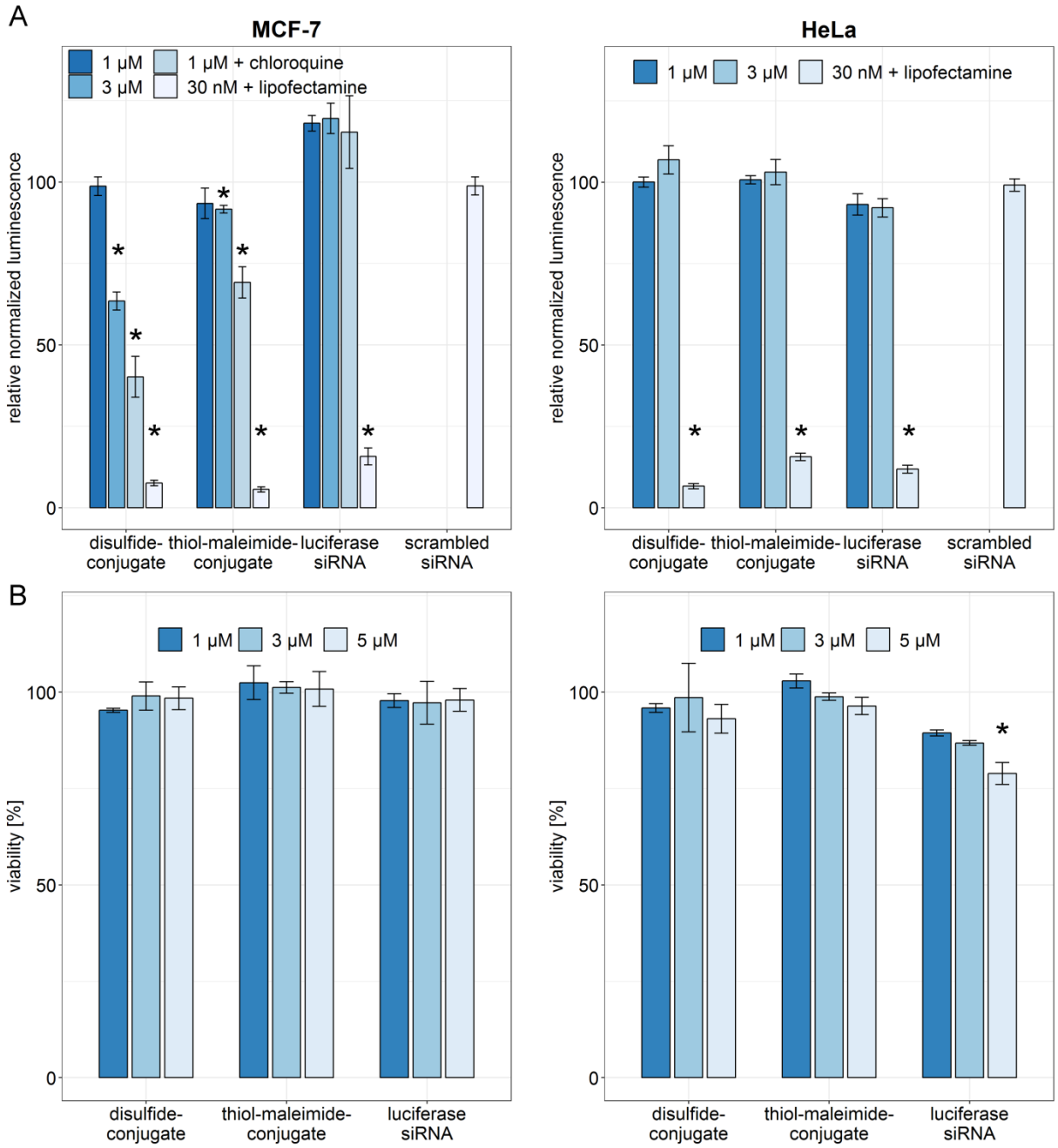


*Figure 7: Gene silencing and cell viability of EpCAM-positive MCF-7 cells and control EpCAM-low HeLa cells after treatment with bioconjugates. A: Luciferase reporter cell lines were used for evaluation of gene silencing of firefly luciferase targeted siRNA-conjugates. Cells were incubated with conjugates (in the presence or absence of 62.5 µM chloroquine) in cell culture*

ACCEPTED MANUSCRIPT

*medium containing 10% FBS for 48 h. Cells were lysed and luminescence signals were evaluated after addition of luciferin. Data are means ± s.d., n = 3, *: p<0.05. B, Cell viability after 24 h incubation with bioconjugates measured by a formazan assay. Data are mean s± s.d., n=3, *: p<0.05.*

As shown in Figure 7, the luminescence reporter assay analysis of disulfide-linked bioconjugates indicated a significant decrease of the luminescence signal to 62%, whereas the more stable thiol-maleimide-linked bioconjugate showed only a minor gene silencing effect in MCF-7 cells (Figure 7A). In contrast, no decrease of luminescence signal was detectable for either disulfide- or thiol-maleimide-linked conjugate in HeLa cells (Figure 7A). These results confirm the EpCAM-specificity, but also highlight a rather low silencing activity. Lipoplex-mediated transfection of conjugates proved that they are intrinsically capable of inducing gene silencing to the same extent as free siRNA, and a scrambled siRNA failed to induce silencing. Addition of chloroquine, an endosomolytic agent, improved gene silencing activity approx. 2-fold for the disulfide-conjugate, and enables silencing with the thiol-maleimide conjugate. Thus, a lack of effective cytosolic concentration, caused by uptake into endosomal compartments and poor endosomal escape, is obviously responsible for the moderate gene silencing effects. The fact that the cleavable disulfide-linked conjugate shows higher silencing activity indicates that the released oligonucleotide itself, butnot the intact conjugate is delivered to the cytoplasm, albeit at low levels.

**Viability assay**

A possible impact on cell viability and proliferation was investigated by a formazan-based assay on MCF-7 and HeLa cells after incubation with the bioconjugates. For all conjugates, no

ACCEPTED MANUSCRIPT

significant signal reduction was found at any concentration (Figure 7B) for MCF-7. A slight reduction of HeLa cell viability was detected for the triazole-conjugate at high concentrations.

## Discussion

Sufficient intracellular delivery still constitutes a major hurdle in the use of therapeutic oligonucleotides for medical applications, in particular when targeting diseased tissues other than the liver [1, 10, 21]. Receptor-specific uptake appears to be an attractive strategy for increasing intracellular delivery of antisense and siRNA oligonucleotides. For effective binding and internalization, appropriate ligands with high receptor affinity and selectivity are essential [4]. Designed Ankyrin Repeat Proteins (DARPins) bind with similar affinity and selectivity as antibodies, but they are devoid of posttranslational modifications, have high chemical and thermal stability, can easily be produced in high yields in bacterial expression systems, and allow facile functionalization for site-specific derivatization [12, 35-37]. Overall, the structural and functional properties of DARPins make them attractive options as carriers for receptor-targeted delivery within oligonucleotide bioconjugates. Previously described fusion proteins for charge complexation of the siRNA cargo resulted in receptor-specific *in vitro* silencing, but they aggregate into supramolecular assemblies with a particle size of around 200 nm [19], which might lead to liver targeting, independent of the receptor. The biodistribution of nanoparticles is determined to a large extent by their nanoscale characteristics, such as the EPR effect, and molecular targeting has limited influence [38]. Thus, we hypothesized that molecular DARPin-siRNA bioconjugates have superior targeting properties. We decided to attach the carrier protein covalently to the sense strand, in order to minimize a potential negative influence on recruitment

ACCEPTED MANUSCRIPT

by RISC, for which the antisense strand is essential. While the sense strand was chemically modified by 2'-O-Me pyrimidines and two phosphorothioate linkages to increase stability against enzymatic degradation, the antisense strand was largely unmodified except for a distinct phosphorothioate at the 3'-end, to avoid negative effects on gene silencing efficacy. After successful synthesis and purification of single stranded conjugates, the complete siRNA-DARPin conjugates were produced by strand hybridization of the antisense complement, proceeding even without the need for heating.

We identified specific binding only on EpCAM-positive cells for all bioconjugates, with negligible binding on HeLa cells. Although generally regarded as EpCAM-negative, HeLa expresses a low basal amount of this protein (Supplementary Information and [29, 30]), and the high affinity of DARPins Ec1 and Ec4 for EpCAM resulted in detectable binding to this cell line. Comparison of bioconjugates with the parent Ec1 and Ec4 in flow cytometric analyses with a secondary anti-penta·His antibody showed that the DARPins retained their binding activity and specificity after being tethered to siRNA.

Concentration-dependent assessment of internalization indicated a specific, EpCAM-mediated process. No internalization was observed at 4 °C showing that an active endocytic process is involved, also evidenced by the punctuate pattern. These results are in good accordance with data of effective internalization of EpCAM-specific DARPins by receptor-mediated endocytosis [22]. Additionally, co-staining with a lysosomal marker indicated that all internalised bioconjugates were predominantly localized in lysosomes after 6 hrs. It should be noted that even after several hours, substantial staining of the plasma membrane was observed suggesting a slow endocytic turnover of this receptor by this method (Figure 6). No significant diffuse stain was noticed.

ACCEPTED MANUSCRIPT

The functional examination of productive cellular uptake, i.e. cytosolic escape, by assessing gene silencing of the luciferase reporter gene resulted in moderate activity of the disulfide conjugate, while thiol-maleimide and also triazole conjugates failed to induce silencing to the level observed with the commercial transfection reagent. Similar to other targeting approaches, insufficient endosomal escape is apparently responsible for the moderate silencing activities [10]. Direct transfection of the conjugates showed strong silencing and this underlines the lack of localization to the cytosol as a limiting step. Endosomal destabilization with chloroquine significantly improved gene silencing (Figure 7) to 60 % and 30 % reduction of luminescence for the disulfide and thiol-maleimide conjugate, respectively. This constitutes an at least two-fold increase in silencing efficacy and further corroborates endosomal entrapment subsequent to receptor-mediated uptake as the hurdle for efficient gene silencing. In vitro, silencing was moderate and occurred after incubating cells with 3 µM concentrations, which would be difficult to achieve in tumor tissue in vivo. DARPin-mediated binding to the cell surface receptor is typically already saturated at a ten-fold lower concentration. Therefore, increasing productive uptake into the cytosol after receptor binding would be crucial. Considering necessary and achievable tissue concentrations, recently published data [39] indicated that concentrations of GalNAc siRNA conjugates in rodent livers of about 20-200 nM result in strong silencing, with only a small percentage of that loaded to the RISC. Approximately 2 µM siRNA conjugate concentrations were measured in the liver after dosing 2.5 mg/kg. Although tissue concentrations in other organs are usually lower, bioconjugate concentrations in the high nanomolar range thus appear to be achievable.

Linker stability is an important aspect for any carrier-cargo conjugate. On the one hand, linkers need to be sufficiently stable in circulation to enable intact delivery to the extracellular

ACCEPTED MANUSCRIPT

receptor [40]. For an antibody-drug conjugate linker stability was found to correlate positively with the pharmacologic effect [40]. Conversely, the cargo may need to be removed from the carrier molecule to be effective. In the case of oligonucleotides, few data on the influence of linker stability exists, and it is not sufficiently clear if the carrier needs to be cleaved from the siRNA duplex, whether the whole conjugate might find its way into the cytosol, or if the antisense strand can eventually be recruited directly to the RISC complex. The different results generated with different linker chemistries, including a disulfide designed to be cleaved in endosomal and lysosomal environments with high glutathione concentrations [41], highlights the importance of the carrier-cargo binding. Indeed, the disulfide-linked compound had better silencing efficacy than the more stable conjugates. While cleavage was observed in serum-supplemented solutions (containing glutathione [42]), lower overall cellular internalization, yet significantly stronger gene silencing was induced with the labile-linked conjugate. This indicates that separation, most probably in endosomes, of carrier and cargo is decisive for achieving productive cytosolic delivery, indicating that only the oligonucleotide duplex is translocated to the cytoplasm at some level, but not the whole conjugate. Improved linkages with higher extracellular stability, but rapid cleavage within endosomes might improve silencing potencies of siRNA conjugates.

While cell recognition and endosomal uptake of the DARPin siRNA conjugates are highly specific, intracellular trafficking, in particular endosomal escape leaves space for improvement. Besides linkers optimized for serum stability but endosomal cleavage, strategies for further optimization include incorporation of a biocompatible endosomal destabilization reagent either as an adjuvant or by covalent attachment [43, 44]. Gene silencing effects of bioconjugates could also be improved by selecting receptor systems with better uptake kinetics, particularly faster

ACCEPTED MANUSCRIPT

internalization rates. The hepatocytic asialoglycoprotein protein receptor, which is targeted by successful GalNAc conjugates for siRNA and antisense, is characterized by a rapid recycling time of around 15 min allowing high uptake rates of GalNAc conjugates [10, 45]. Thus, DARPin-siRNA bioconjugates targeting receptors with higher uptake rates and recycling would lead to a faster recycling time and consecutively, higher siRNA concentrations could reach the cytosol. However, precise uptake and intracellular trafficking routes depend on a multitude of factors, many of which are still incompletely understood [46, 47].

## Conclusion

The bioconjugates developed herein serve as prototype and can be easily adapted for different targets at the receptor level (by selecting DARPins for other antigens), and for different genes to be silenced (by using respective siRNA sequences). Our data highlights high *in vitro* cell-type specificity and the beneficial effects of cleavable linkers, while suggesting endosomal escape to be the bottleneck for the development of more efficient targeted siRNA therapeutics. In contrast to other approaches, the bioconjugates and the synthetic procedures presented herein are highly modular, as both targeting protein and effector molecules are homogenous in their structural and biophysical properties, independent of their target. The synthetic methodology and purification and characterization procedures can likewise be adopted for other DARPin-siRNA conjugates and represents a versatile system for receptor-targeted siRNA delivery.

## Acknowledgements

Luciferase-expressing cell lines MCF-7 and HeLa were kindly provided by Manfred Ogris, University of Vienna. The research leading to these results has received support from the

ACCEPTED MANUSCRIPT

Innovative Medicines Initiative Joint Undertaking under grant agreement n° [115363], resources of which are composed of financial contribution from the European Union's Seventh Framework Programme (FP7/2007-2013) and EFPIA companies' in kind contribution. The funder had no role in experimental design data acquisition and interpretation and the decision for publication.

## Declaration of interest: none

## References

[1] C. Lorenzer, M. Dirin, A.-M. Winkler, V. Baumann, J. Winkler, Going beyond the liver: Progress and challenges of targeted delivery of siRNA therapeutics, J. Control. Release, 203 (2015) 1-15. https://doi.org/10.1016/j.jconrel.2015.02.003.

[2] A. Khvorova, J.K. Watts, The chemical evolution of oligonucleotide therapies of clinical utility, Nat. Biotechnol., 35 (2017) 238-248. https://doi.org/10.1038/nbt.3765.

[3] T.S. Zatsepin, Y.V. Kotelevtsev, V. Koteliansky, Lipid nanoparticles for targeted siRNA delivery – going from bench to bedside, Int. J. Nanomed., 11 (2016) 3077-3086. https://doi.org/10.2147/IJN.S106625.

[4] J. Winkler, Oligonucleotide conjugates for therapeutic applications., Ther. Deliv., 4 (2013) 791-809. https://doi.org/10.4155/tde.13.47.

[5] D. Adams, O.B. Suhr, P.J. Dyck, W.J. Litchy, R.G. Leahy, J. Chen, J. Gollob, T. Coelho, Trial design and rationale for APOLLO, a Phase 3, placebo-controlled study of patisiran in patients with hereditary ATTR amyloidosis with polyneuropathy, BMC Neurology, 17 (2017) 181. https://doi.org/10.1186/s12883-017-0948-5.

[6] Y. Huang, Preclinical and Clinical Advances of GalNAc-Decorated Nucleic Acid Therapeutics, Mol. Ther. Nucleic Acids, 6 (2017) 116-132. https://doi.org/10.1016/j.omtn.2016.12.003.

[7] E.I. Park, Y. Mi, C. Unverzagt, H.-J. Gabius, J.U. Baenziger, The asialoglycoprotein receptor clears glycoconjugates terminating with sialic acidα2,6GalNAc, Proc. Natl. Acad. Sci. U. S. A., 102 (2005) 17125-17129. https://doi.org/10.1073/pnas.0508537102.

ACCEPTED MANUSCRIPT

[8] A.L. Schwartz, S.E. Fridovich, H.F. Lodish, Kinetics of internalization and recycling of the asialoglycoprotein receptor in a hepatoma cell line, J. Biol. Chem., 257 (1982) 4230-4237.

[9] A.A. D'Souza, P.V. Devarajan, Asialoglycoprotein receptor mediated hepatocyte targeting — Strategies and applications, J. Control. Release, 203 (2015) 126-139. https://doi.org/10.1016/j.jconrel.2015.02.022.

[10] S.F. Dowdy, Overcoming cellular barriers for RNA therapeutics, Nat. Biotechnol., 35 (2017) 222-229. https://doi.org/10.1038/nbt.3802.

[11] A. Beck, J.M. Reichert, Antibody-drug conjugates, MAbs, 6 (2014) 15-17. https://doi.org/10.4161/mabs.27436.

[12] A. Plückthun, Designed Ankyrin Repeat Proteins (DARPins): Binding Proteins for Research, Diagnostics, and Therapy, Annu. Rev. Pharmacol. Toxicol., 55 (2015) 489-511. https://doi.org/10.1146/annurev-pharmtox-010611-134654.

[13] R. Tamaskovic, M. Simon, N. Stefan, M. Schwill, A. Plückthun, Designed ankyrin repeat proteins (DARPins): from research to therapy, in: K.D. Wittrup, L.V. Gregory (Eds.) Methods Enzymol., Academic Press, 2012, pp. 101-134.

[14] R.C. Münch, M.D. Mühlebach, T. Schaser, S. Kneissl, C. Jost, A. Plückthun, K. Cichutek, C.J. Buchholz, DARPins: An Efficient Targeting Domain for Lentiviral Vectors, Mol. Ther., 19 (2011) 686-693. https://doi.org/10.1038/mt.2010.298.

[15] K. Friedrich, J.R.H. Hanauer, S. Prüfer, R.C. Münch, I. Völker, C. Filippis, C. Jost, K.-M. Hanschmann, R. Cattaneo, K.-W. Peng, A. Plückthun, C.J. Buchholz, K. Cichutek, M.D. Mühlebach, DARPin-targeting of Measles Virus: Unique Bispecificity, Effective Oncolysis, and Enhanced Safety, Mol. Ther., 21 (2013) 849-859. https://doi.org/10.1038/mt.2013.16.

[16] M. Schmid, P. Ernst, A. Honegger, M. Suomalainen, M. Zimmermann, L. Braun, S. Stauffer, C. Thom, B. Dreier, M. Eibauer, A. Kipar, V. Vogel, U.F. Greber, O. Medalia, A. Plückthun, Adenoviral vector with shield and adapter increases tumor specificity and escapes liver and immune control, Nat. Commun., 9 (2018) 450. https://doi.org/10.1038/s41467-017-02707-6.

[17] M. Simon, U. Zangemeister-Wittke, A. Plückthun, Facile double-functionalization of designed ankyrin repeat proteins using click and thiol chemistries, Bioconjug. Chem., 23 (2012) 279-286. https://doi.org/10.1021/bc200591x.

ACCEPTED MANUSCRIPT

[18] M. Simon, R. Frey, U. Zangemeister-Wittke, A. Plückthun, Orthogonal Assembly of a Designed Ankyrin Repeat Protein–Cytotoxin Conjugate with a Clickable Serum Albumin Module for Half-Life Extension, Bioconjug. Chem., 24 (2013) 1955-1966. https://doi.org/10.1021/bc4004102.

[19] J. Winkler, P. Martin-Killias, A. Plueckthun, U. Zangemeister-Wittke, EpCAM-targeted delivery of nanocomplexed siRNA to tumor cells with designed ankyrin repeat proteins, Mol. Cancer Ther., 8 (2009) 2674-2683. https://doi.org/10.1158/1535-7163.MCT-09-0402.

[20] R.L. Juliano, X. Ming, O. Nakagawa, Cellular uptake and intracellular trafficking of antisense and siRNA oligonucleotides, Bioconjug. Chem., 23 (2012) 147-157. https://doi.org/10.1021/bc200377d.

[21] R.L. Juliano, The delivery of therapeutic oligonucleotides, Nucleic Acids Res., 44 (2016) 6518-6548. https://doi.org/10.1093/nar/gkw236.

[22] N. Stefan, P. Martin-Killias, S. Wyss-Stoeckle, A. Honegger, U. Zangemeister-Wittke, A. Plückthun, DARPins recognizing the tumor-associated antigen EpCAM selected by phage and ribosome display and engineered for multivalency, J. Mol. Biol., 413 (2011) 826-843. https://doi.org/10.1016/j.jmb.2011.09.016.

[23] N. Stefan, M. Zimmermann, M. Simon, U. Zangemeister-Wittke, A. Pluckthun, Novel Prodrug-Like Fusion Toxin with Protease-Sensitive Bioorthogonal PEGylation for Tumor Targeting, Bioconjug. Chem., 25 (2014) 2144-2156. https://doi.org/10.1021/bc500468s.

[24] S. Shah, S.H. Friedman, An ESI-MS method for characterization of native and modified oligonucleotides used for RNA interference and other biological applications, Nat. Prot., 3 (2008) 351-356. https://doi.org/10.1038/nprot.2007.535.

[25] B. Su, A. Cengizeroglu, K. Farkasova, J.R. Viola, M. Anton, J.W. Ellwart, R. Haase, E. Wagner, M. Ogris, Systemic TNF[alpha] Gene Therapy Synergizes With Liposomal Doxorubicine in the Treatment of Metastatic Cancer, Mol. Ther., 21 (2013) 300-308. https://doi.org/10.1038/mt.2012.229.

[26] R. Wu, E. Wyatt, K. Chawla, M. Tran, M. Ghanefar, M. Laakso, C.L. Epting, H. Ardehali, Hexokinase II knockdown results in exaggerated cardiac hypertrophy via increased ROS production, EMBO Mol. Med., 4 (2012) 633-646. https://doi.org/10.1002/emmm.201200240.

ACCEPTED MANUSCRIPT

[27] S.K. Wetzel, G. Settanni, M. Kenig, H.K. Binz, A. Plückthun, Folding and Unfolding Mechanism of Highly Stable Full-Consensus Ankyrin Repeat Proteins, J. Mol. Biol., 376 (2008) 241-257.

[28] A.D. Baldwin, K.L. Kiick, Tunable Degradation of Maleimide–Thiol Adducts in Reducing Environments, Bioconjug. Chem., 22 (2011) 1946-1953. https://doi.org/10.1021/bc200148v.

[29] Human Protein Atlas, https://www.proteinatlas.org, 2018.

[30] M. Uhlén, L. Fagerberg, B.M. Hallström, C. Lindskog, P. Oksvold, A. Mardinoglu, Å. Sivertsson, C. Kampf, E. Sjöstedt, A. Asplund, I. Olsson, K. Edlund, E. Lundberg, S. Navani, C.A.-K. Szigyarto, J. Odeberg, D. Djureinovic, J.O. Takanen, S. Hober, T. Alm, P.-H. Edqvist, H. Berling, H. Tegel, J. Mulder, J. Rockberg, P. Nilsson, J.M. Schwenk, M. Hamsten, K. von Feilitzen, M. Forsberg, L. Persson, F. Johansson, M. Zwahlen, G. von Heijne, J. Nielsen, F. Pontén, Tissue-based map of the human proteome, Science, 347 (2015). https://doi.org/10.1126/science.1260419.

[31] A. Martowicz, G. Spizzo, G. Gastl, G. Untergasser, Phenotype-dependent effects of EpCAM expression on growth and invasion of human breast cancer cell lines, BMC Cancer, 12 (2012) 501. https://doi.org/10.1186/1471-2407-12-501.

[32] S. Aubry, F. Burlina, E. Dupont, D. Delaroche, A. Joliot, S. Lavielle, G. Chassaing, S. Sagan, Cell-surface thiols affect cell entry of disulfide-conjugated peptides, FASEB J., 23 (2009) 2956-2967. https://doi.org/10.1096/fj.08-127563.

[33] P.R. Moody, E.J. Sayers, J.P. Magnusson, C. Alexander, P. Borri, P. Watson, A.T. Jones, Receptor Crosslinking: A General Method to Trigger Internalization and Lysosomal Targeting of Therapeutic Receptor:Ligand Complexes, Mol. Ther., 23 (2015) 1888-1898. https://doi.org/10.1038/mt.2015.178.

[34] W.H.I.V. Humphries, C.J. Szymanski, C.K. Payne, Endo-Lysosomal Vesicles Positive for Rab7 and LAMP1 Are Terminal Vesicles for the Transport of Dextran, PLOS One, 6 (2011) e26626. https://doi.org/10.1371/journal.pone.0026626.

[35] W.P.R. Verdurmen, M. Mazlami, A. Plückthun, A quantitative comparison of cytosolic delivery via different protein uptake systems, Sci. Rep., 7 (2017) 13194. https://doi.org/10.1038/s41598-017-13469-y.

ACCEPTED MANUSCRIPT

[36] H.K. Binz, P. Amstutz, A. Kohl, M.T. Stumpp, C. Briand, P. Forrer, M.G. Grutter, A. Plückthun, High-affinity binders selected from designed ankyrin repeat protein libraries, Nat. Biotechnol., 22 (2004) 575-582. https://doi.org/10.1038/nbt962.

[37] C. Zahnd, M. Kawe, M.T. Stumpp, C. de Pasquale, R. Tamaskovic, G. Nagy-Davidescu, B. Dreier, R. Schibli, H.K. Binz, R. Waibel, A. Pluckthun, Efficient tumor targeting with high-affinity designed ankyrin repeat proteins: effects of affinity and molecular size, Cancer Res., 70 (2010) 1595-1605. https://doi.org/10.1158/0008-5472.CAN-09-2724.

[38] N. Bertrand, J. Wu, X. Xu, N. Kamaly, O.C. Farokhzad, Cancer nanotechnology: The impact of passive and active targeting in the era of modern cancer biology, Adv. Drug Deliv. Rev., 66 (2014) 2-25. https://doi.org/10.1016/j.addr.2013.11.009.

[39] J.K. Nair, H. Attarwala, A. Sehgal, Q. Wang, K. Aluri, X. Zhang, M. Gao, J. Liu, R. Indrakanti, S. Schofield, P. Kretschmer, C.R. Brown, S. Gupta, J.L.S. Willoughby, J.A. Boshar, V. Jadhav, K. Charisse, T. Zimmermann, K. Fitzgerald, M. Manoharan, K.G. Rajeev, A. Akinc, R. Hutabarat, M.A. Maier, Impact of enhanced metabolic stability on pharmacokinetics and pharmacodynamics of GalNAc-siRNA conjugates, Nucleic Acids Res., 45 (2017) 10969-10977. https://doi.org/10.1093/nar/gkx818.

[40] M. Dorywalska, P. Strop, J.A. Melton-Witt, A. Hasa-Moreno, S.E. Farias, M. Galindo Casas, K. Delaria, V. Lui, K. Poulsen, C. Loo, S. Krimm, G. Bolton, L. Moine, R. Dushin, T.-T. Tran, S.-H. Liu, M. Rickert, D. Foletti, D.L. Shelton, J. Pons, A. Rajpal, Effect of Attachment Site on Stability of Cleavable Antibody Drug Conjugates, Bioconjug. Chem., 26 (2015) 650-659. https://doi.org/10.1021/bc5005747.

[41] J. Lu, F. Jiang, A. Lu, G. Zhang, Linkers Having a Crucial Role in Antibody-Drug Conjugates, Int. J. Mol. Sci., 17 (2016) 561. https://doi.org/10.3390/ijms17040561.

[42] J.C. Livesey, D.J. Reed, Measurement of glutathione-protein mixed disulfides, Int. J. Radiat. Oncol. Biol. Phys., 10 (1984) 1507-1510. https://doi.org/10.1016/0360-3016(84)90491-7.

[43] J. Gilleron, P. Paramasivam, A. Zeigerer, W. Querbes, G. Marsico, C. Andree, S. Seifert, P. Amaya, M. Stöter, V. Koteliansky, H. Waldmann, K. Fitzgerald, Y. Kalaidzidis, A. Akinc, M.A. Maier, M. Manoharan, M. Bickle, M. Zerial, Identification of siRNA delivery enhancers by a chemical library screen, Nucleic Acids Res., 43 (2015) 7984-8001. https://doi.org/10.1093/nar/gkv762.

ACCEPTED MANUSCRIPT

[44] M.F. Osborn, J.F. Alterman, M. Nikan, H. Cao, M.C. Didiot, M.R. Hassler, A.H. Coles, A. Khvorova, Guanabenz (Wytensin™) selectively enhances uptake and efficacy of hydrophobically modified siRNAs, Nucleic Acids Res., 43 (2015) 8664–8672. https://doi.org/10.1093/nar/gkv942.

[45] J.K. Nair, J.L.S. Willoughby, A. Chan, K. Charisse, M.R. Alam, Q. Wang, M. Hoekstra, P. Kandasamy, A.V. Kel'in, S. Milstein, N. Taneja, J. O'Shea, S. Shaikh, L. Zhang, R.J. van der Sluis, M.E. Jung, A. Akinc, R. Hutabarat, S. Kuchimanchi, K. Fitzgerald, T. Zimmermann, T.J.C. van Berkel, M.A. Maier, K.G. Rajeev, M. Manoharan, Multivalent N-Acetylgalactosamine-Conjugated siRNA Localizes in Hepatocytes and Elicits Robust RNAi-Mediated Gene Silencing, J. Am. Chem. Soc., 136 (2014) 16958-16961. https://doi.org/10.1021/ja505986a.

[46] J. R.L., Intracellular Trafficking and Endosomal Release of Oligonucleotides: What We Know and What We Don't, Nucl. Acids Therap., 28 (2018) 166-177. https://doi.org/10.1089/nat.2018.0727.

[47] G. Sahay, W. Querbes, C. Alabi, A. Eltoukhy, S. Sarkar, C. Zurenko, E. Karagiannis, K. Love, D. Chen, R. Zoncu, Y. Buganim, A. Schroeder, R. Langer, D.G. Anderson, Efficiency of siRNA delivery by lipid nanoparticles is limited by endocytic recycling, Nat. Biotechnol., 31 (2013) 653-658. https://doi.org/10.1038/nbt.2614.

ACCEPTED MANUSCRIPT